Russian Chemical Reviews **64** (8) 719 – 729 (1995)
©1995 Russian Academy of Sciences and Turpion Ltd

UDC 546.3; 546.55; 548.3; 548.537

Complex oxides with coherent intergrowth structures

A M Abakumov, E V Antipov, L M Kovba, E M Kopnin, S N Putilin, R V Shpanchenko

Contents

I. Introduction 719
II. Structures with alternation of fragments with different structures along the fourfold axis 720
III. Intergrowth structures with alternation of fragments along the threefold axis of the perovskite subcell 724
IV. Conclusion 728

Abstract. The review deals with the characteristic features of the formation of certain complex perovskite-like oxides. In the crystal structures of these compounds, it is possible to differentiate fragments with different structures, which alternate along the three-fold or four-fold axis of the perovskite sublattice. This approach has been applied successfully to the synthesis of a large number of new complex transition metal oxides, in particular those belonging to the family of Hg-containing high-temperature superconductors with the highest transition temperatures for superconduction. The bibliography includes 79 references.

I. Introduction

Fragments with different structures, for example blocks of the perovskite ($CaTiO_3$), sodium chloride (NaCl), and fluorite (CaF_2) types or individual layers alternating along the large period of the unit cell may be conventionally differentiated in the structures of many complex oxides. In many instances, the differentiation of such fragments is conventional [for example, the differentiation of the (TiO_2) layers in the perovskite structure]. However, in the structures of the superconducting complex copper oxides, which will be considered in the second section of the present review, the differentiation of the (CuO_2) layers is justified, since the Cu – O distance in these layers is much shorter than the distances between the atoms of the neighbouring layers. A necessary condition for the formation of structures consisting of alternating blocks is the geometrical compatibility of fragments with different structures, for example in the *ab* plane. The cubic unit cell parameters a of oxides with structures of the NaCl and CaF_2 types are in the range from 5.4 to 5.7 Å. The cation–cation distance in these structures is close to the corresponding distances in perovskite-type structures — 3.8 – 4.2 Å ($a_{NaCl} \approx a_{fl} \approx \sqrt{2}a_{per}$). The face-centred unit cells of the NaCl and fluorite types can be transformed into tetragonal body-centred cells with the parameter a close to a_{per}. We may note that the motif in the arrangement of the cations in the perovskite structure and in the transformed cells of the fluorite and NaCl types is the same, but the coordinates of the oxygen atoms are different (Fig. 1).

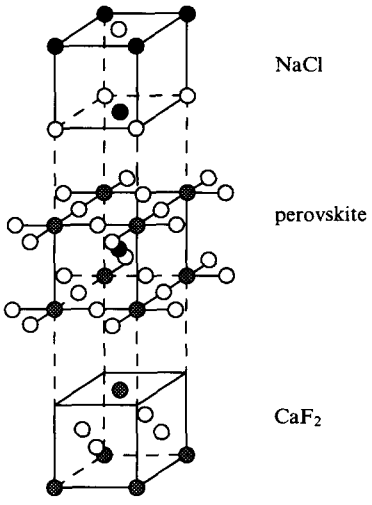


Figure 1. Schematic illustration of the formation of intergrowth structures for the alternation of NaCl- or fluorite-type blocks and (CuO_2) layers along the fourfold axis.

The third section of the review deals with compounds in the structures of which the common elements of the fragments are close-packed layers. In this case, the coalesceing fragments are oriented at right angles to the threefold axis of the perovskite sublattice. An obligatory condition for the formation of coherent intergrowth structures is also the chemical compatibility of the ions entering into their composition (for example, the situation where powerful oxidants and reductants are not present simultaneously) and the electrical neutrality of the unit cell. One should also note that the consideration of structures in inorganic chemistry as sequences of simpler structures arranged in a definite order is to some extent analogous to the description of homologous series of organic compounds. The difference consists in the fact that the alternating elements in the latter case are isolated groups of atoms, whereas in inorganic compounds these are layers or blocks of infinite extent in two directions.

The use of such a treatment of the structures makes it possible to predict the feasibility of synthesising new compounds having the necessary structural fragments giving rise to unique physical properties. For example, we have used this to synthesise new superconducting complex copper oxides.

A M Abakumov, E V Antipov, L M Kovba, E M Kopnin, S N Putilin, R V Shpanchenko Faculty of Chemistry, Lomonosov Moscow State University, Vorob'evy gory, 119899 Moscow, Russian Federation. Fax (7-095) 939 09 98

Received 7 April 1995
Uspekhi Khimii **64** (8) 769 – 779 (1995); translated by A K Grzybowski

II. Structures with alternation of fragments with different structures along the fourfold axis

1. Complex copper oxides having the general formula A_2BO_4

The simplest coherent intergrowth structure is that of K_2NiF_4. Numerous complex lanthanide and transition element oxides crystallise in this structural type.[1,2] The structure contains fragments of the perovskite and NaCl types (Fig. 2). The structure of K_2NiF_4 can be represented schematically as the following arrangement of layers along the threefold axis:

$$\cdots(NiF_2)-(KF)-(FK)-(F_2Ni)-(FK)-(KF)-(NiF_2)\cdots$$
$$\longleftarrow\quad c \quad\longrightarrow$$

where $c \approx 3a_{per}$.

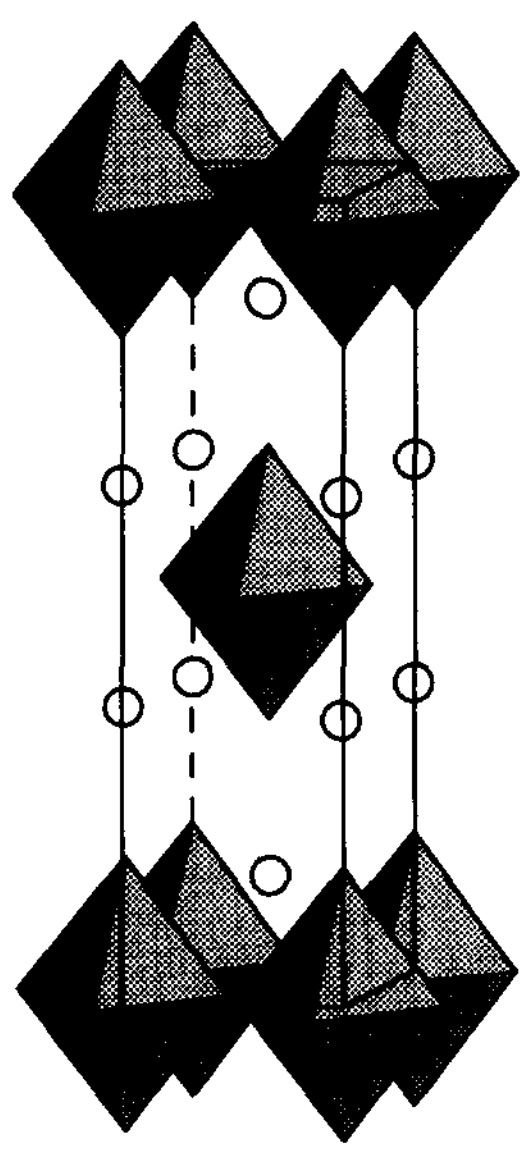


Figure 2. *Coordination polyhedra of the nickel atoms in the* K_2NiF_4 structural type.

The atoms in the (KF) and (FK) as well as (NiF_2) and (F_2Ni) layers are displaced relative to one another by a $\frac{1}{2}(\vec{a}+\vec{b})$ translation. The coordination number (CN) of the A cation in this structure is reduced from 12 to 9, in contrast to the perovskite structure. Among lanthanide cuprates, only La_2CuO_4 (*T*-phase) crystallises in the K_2NiF_4 structural type and its low-temperature modification has an orthorhombically distorted structure.[3] The substitution of La^{3+} by alkaline earth metal cations in La_2CuO_4 leads to the stabilisation of the tetragonal modification[4,5] — for example, the crystal lattice of the $La_{2-x}Sr_xCuO_{4-\delta}$ solid solution becomes tetragonal for $x \geqslant 0.1$,[4] the solid solution possessing superconducting properties with $T_c^{max} = 38$ K for $x = 0.15$.[6] The coordination polyhedron of copper is an octahedron distorted as a consequence of the Jahn–Teller effect.

The cuprates R_2CuO_4 of lanthanides having the smallest ionic radii (R = Pr – Gd) crystallises in another structural type — Nd_2CuO_4 (*T'*-phases).[7] The structures of these phases differ from that of La_2CuO_4 only by the arrangement of the oxygen atoms in the unit cell. The coordination number of the lanthanide is reduced to 8, while the coordination polyhedron of copper in the *T'*-phases is a square ($d_{Cu-O} = 1.95 - 1.98$ Å).[8,9] The structures of the *T'*-phases can be represented as a result of the alternation of the (R_2O_2) fluorite fragments and the (CuO_2) layers along the *c* axis of the unit cell (Fig. 3). It has been established that, when the trivalent lanthanide cations are replaced by tetravalent ones (Ce^{4+}, Th^{4+}),

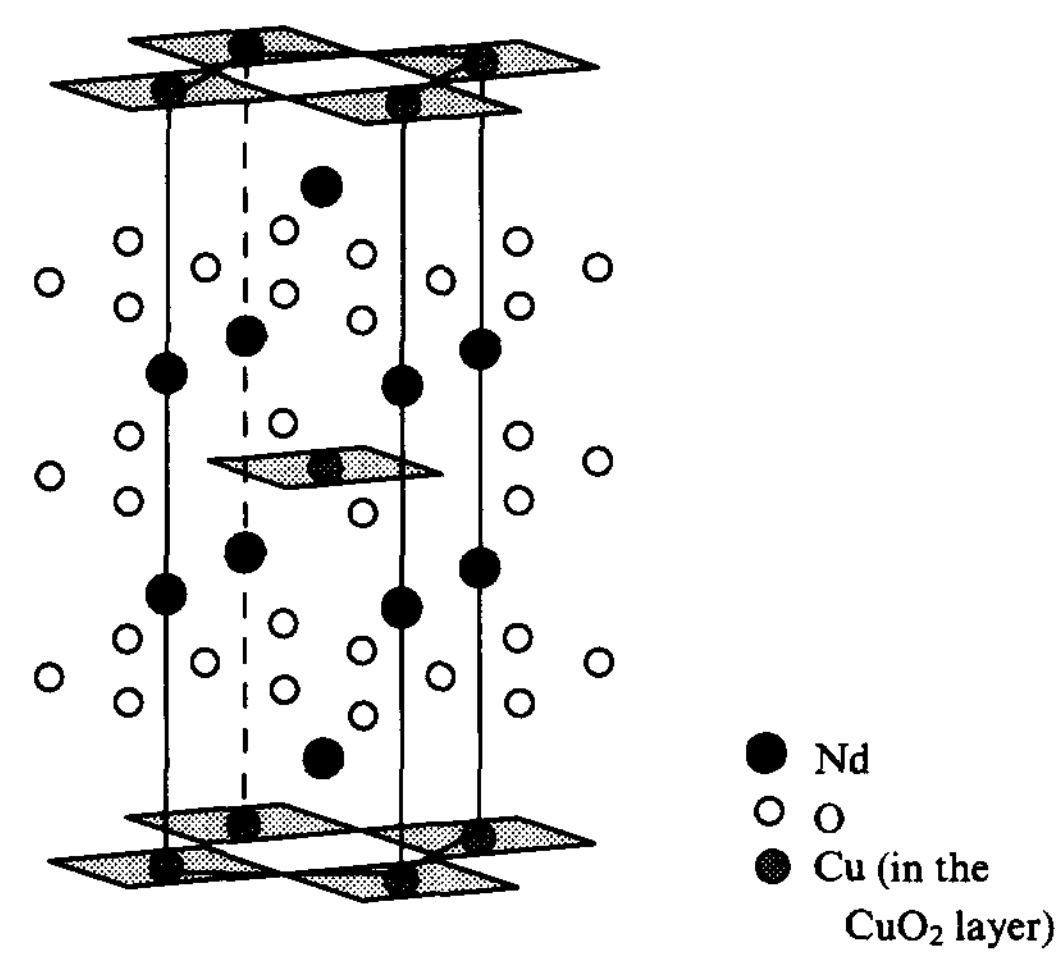


Figure 3. The crystal structure of the *T'*-phases. The coordination polyhedron of the copper atoms is a square.

the majority of the *T'*-phases (R = Pr – Eu) pass to the superconducting state, electrons being the charge carriers, while $T_c^{max} = 24$ K for R = Nd or Pr.[10] The synthesis at atmospheric pressure leads to the formation of lanthanide cuprates (R = Dy – Tm, Y) with a different composition $(R_2Cu_2O_5)$, in the structures of which the lanthanide element has a coordination number of 6.[11] Compounds of the same lanthanide isostructural with Nd_2CuO_4 have been obtained only by employing high isostatic pressures (50 – 80 kbar).[12]

The complex copper oxides $(La, R)_2CuO_{4-\delta}$ (R = Gd, Tb, or Dy) with specific ratios of lanthanum and the other lanthanide crystallise in a new structural type — the *T**-phase. In the structures of these phases, the (CuO_2) layers alternate with blocks of the fluorite and NaCl types (Fig. 4). In the structures of the *T**-phases, it is possible to differentiate cationic sites in the fluorite (CN = 8) and NaCl-type (CN = 9) fragments. An important condition for the preparation of the above compounds is therefore the presence of two different lanthanide cations, which populate these sites in an ordered manner. The coordination polyhedron of the copper ions is a tetragonal pyramid extended along the fourfold axis. The addition of the alkaline earth metal

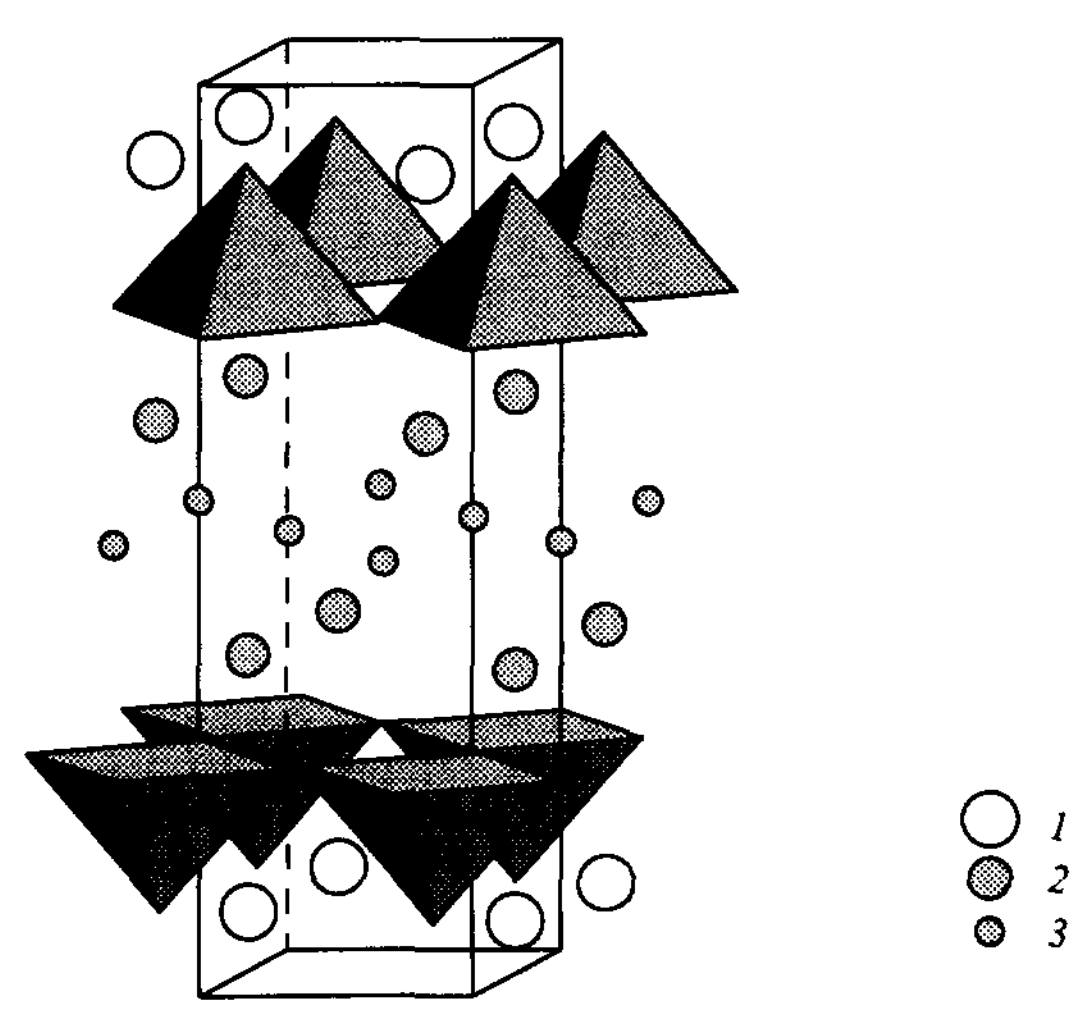


Figure 4. The crystal structure of *T**-phases. The coordination polyhedra of the copper atoms, the cations in the NaCl (*1*) and fluorite (*2*) blocks, and the oxygen atoms (*3*) are shown.

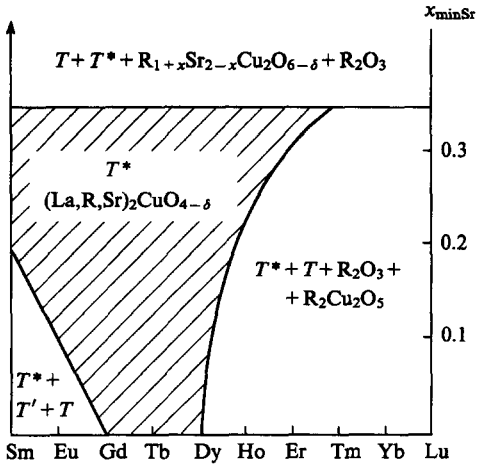


Figure 5. Dependence of the minimum concentration of strontium on the nature of the lanthanide for solid solutions with the structure of the T^*-phases.

cations Sr^{2+} or Ba^{2+} makes it possible to obtain the T^*-phases also with other lanthanide elements. Such phases have been obtained in systems with R = Sm – Lu and Y (Fig. 5).[13–16]

It is noteworthy that the X-ray diffraction patterns of the T-, T'- and T^*-phases are very similar. This is due to the fact that the cations in the structures of the phases populate the same positions. However, the unit cell of the T^*-phases is primitive, in contrast to the body-centred cells of the T- and T'-phases. Furthermore, the ratios of the unit cell parameters of the above phases differ significantly: the ratio $c/3a$ is ~ 1.15 for the T-phases, $\sim 1.06 - 1.08$ for the T^*-phases, and ~ 1.02 for the T'-phases.

It has been suggested on the basis of the analysis of the tolerance factors $t(t = d_{A-O}/\sqrt{2}d_{B-O})$ for a large number of the compounds A_2BO_4 that the structures of phases with a given composition can be predicted from the value of t.[17] The authors established that $0.87 \leqslant t \leqslant 0.99$ for the T-phases and $0.83 \leqslant t \leqslant 0.855$ for the T'-phases, while the T^*-phases exist (if they are formed in the given system) within the very narrow range $0.855 \leqslant t \leqslant 0.87$. Naturally, in the latter case at least two A-type cations are needed for the ordered population of two different positions.

Undoubtedly the employment of the tolerance factor is useful and in many cases makes it possible to predict correctly the structures of the compounds. However, the limitations and disadvantages of this method must be noted. Firstly, the above model presupposes the purely ionic character of the A–O and B–O bonds, which is not quite correct when B is a transition element, since in this case the B–O bond is to a large extent covalent. Secondly, the model ignores the electronic structure of the B cations. It is well known that the T'-phases are formed only for $B = Cu^{2+}$, whereas the square coordination is characteristic also of other cations (Ni^{2+}, Pt^{2+}, etc.). However, the compound Gd_2NiO_4, for example, which should have the structure of a T'-phase in terms of the value of t, has in fact the structure of a T-phase.[18] Thirdly, with the aid of this model it is impossible to explain why a compound with the same cationic composition subjected to different heat treatment conditions has different structures. For example, the compound $La_{1.2}Dy_{0.7}Ce_{0.1}CuO_{4+\delta}$, synthesised at $p_{O_2} = 1$ bar, has the structure of a T^*-phase, whereas after annealing under a nitrogen atmosphere a T'-phase is formed.[19]

In our view, apart from the purely geometrical criteria, it is also necessary to take into account electronic structure factors. For example, Ni-containing compounds with the structure of a T'-phase are not formed, apparently because the pairing energy of the e_g electrons is higher for the Ni^{2+} cation with the $3d^8$ electronic configuration than the energy gain in the subsequent removal of degeneracy when the environment of Ni^{2+} is altered to the square form. Furthermore, the geometrical dimensions of the (CuO_2) layer also depend on the electronic factors. We shall consider this in greater detail.

The size of the perovskite block in the *ab* plane is to a large extent determined by the length of the Cu – O bonds in the (CuO_2) layer. The length of these bonds is determined by the degree of filling of the σ^*-zone, formed mainly as a result of the overlap of the $3d_{x^2-y^2}$ orbitals of copper and the $2p_{x,y}$ orbitals of oxygen. An increase in the degree of filling of the σ^*-zone (an increase in the height of the Fermi level), which corresponds to a decrease in the formal oxidation state of copper, leads to an increase in the length of the Cu–O bonds in the (CuO_2) layer. When electrons are removed from the σ^*-zone (this corresponds to an increase in the formal oxidation state of copper), the lengths of these bonds diminish. The degree of filling of the above zone can therefore determine to a large extent whether the perovskite and other structural fragments have common dimensions. It can be altered by the heterovalent substitution of the cations in the structure and by varying the heat treatment atmosphere.

In the La–R–Cu–O systems, T^*-phases are formed only for R = Gd – Dy. The lanthanide atoms in the structure of the T^*-phase populate in an ordered manner two different crystallographic sites. For the lanthanides at the beginning of the series with ionic radii similar to that of lanthanum, such ordering does not occur. Instead, the formation of extended regions of solid solutions with T'-phase structures is energetically more favourable. When R = Ho – Lu and Y, an appreciable decrease in the effective radius of the cation in the fluorite fragment leads to the disappearance of common dimensions between this fragment and the (CuO_2) layer. As a result, the corresponding T^*-phases are not formed.

However, the partial substitution of La^{3+} by Sr^{2+} or Ba^{2+} in the NaCl-type fragment leads to the stabilisation of the T^*-phase structure. It has been established in relation to the solid solutions $La_{1.2-x}Dy_{0.8}M_xCuO_{4-\delta}$ (M = Sr or Ba) that such substitution leads to an increase in the average formal oxidation states of copper.[16] The Cu–O distance then diminishes in the (CuO_2) layer, which is reflected by a decrease in the unit cell parameter a with increase in the concentration of the alkaline earth metal cations despite the fact that their ionic radii are greater than that of La^{3+}.

With decrease in the R^{3+} radius in the series of lanthanides, there is an increase in the oxygen nonstoichiometry indices of the compounds obtained (Table 1). This results in an increase in the concentration of electrons in the antibonding σ^*-zone (or in the 'reduction' of copper), which should be accompanied by an increase in the Cu–O distance in the (CuO_2) layer. Thus, the decrease in the size of the fluorite fragment owing to the decrease in the ionic radius of the lanthanide is accompanied by an increase in the linear dimensions of the (CuO_2) layer and the T^*-phase is not formed as a result. However, the addition of an alkaline earth element, accompanied by a decrease in the equatorial Cu–O distance as a consequence of the 'oxidation' of the (CuO_2) layer, makes it possible to stabilise the T^*-phase structure also in systems with R = Ho – Lu and Y. It is noteworthy that the minimum Sr concentration required in the given series of lanthanides increases steadily with decrease in the ionic radii of the latter (Fig. 5).

Table 1. The unit cell parameters (a), the oxygen nonstoichiometry indices (δ), and the formal oxidation states of copper (V_{Cu}) for the T^*-phases $LaR_{0.8}Sr_{0.2}CuO_{4-\delta}$ (R = Sm, Gd, or Ho).

Compound	a/Å	δ	V_{Cu}
$LaSm_{0.8}Sr_{0.2}CuO_{4-\delta}$	3.8710(4)	0.06	2.08
$LaGd_{0.8}Sr_{0.2}CuO_{4-\delta}$	3.8583(2)	0.08	2.04
$LaHo_{0.8}Sr_{0.2}CuO_{4-\delta}$	3.8375(4)	0.11	1.98

In the systems with R = Sm and Eu, the addition of strontium or barium also leads to a decrease in the Cu–O distance in the (CuO_2) layer, whereupon the resulting 'contraction' of the structure in the *ab* plane leads to a decrease in the M–O interatomic distances for the cations in the fluorite fragment. The filling of the cationic sites in the latter by lanthanum atoms becomes energetically unfavourable. This results in the formation of a T^*-phase structure in which the La and Sr atoms populate statistically the cationic sites in a NaCl-type block, while the Sm and La atoms populate the sites in the fluorite fragment.

As noted above, the degree of filling of the σ^*-zone depends on the oxygen pressure employed in the synthesis. For example, after synthesis at 950 °C in a stream of oxygen, $La_{1.5}Nd_{0.5}CuO_{4-\delta}$ has a *T*-phase structure ($\delta = -0.01$), whereas heat treatment under less oxidising conditions (1050 °C, air) leads to a phase transformation with formation of a T'-phase ($\delta = +0.02$).[19] The decrease in the Cu–O distance in the (CuO_2) layer and the stablisation of the phase with a smaller unit cell parameter *a* during synthesis under an oxidising atmosphere are a consequence in this case of the increase in the formal oxidation state of copper.

2. Compounds of the 223 and 1222 types

Another example of compounds in the structures of which it is possible to differentiate fragments with different structures are the 223 phases. The first representatives of this family of phases having the composition $(R_{1-x}Ba_x)_2(R'_{1-y}Ce_y)_2Cu_3O_{8+\delta}$ ($R = R'$ = Nd, Sm, or Eu, $x = 0.67$, $y = 0.33$) have been obtained by Japanese investigators.[20] The structure of these phases (Fig. 6) is derived from the tetragonal modification of the 123 phases $(RBa_2Cu_3O_{7-\delta})$, but the $(R'_2O_2)^{n+}$ fluorite fragment is located between the (CuO_2) layers instead of the $(R\square)^{3+}$ layer. This results in the doubling of the unit cell parameters *c*, since in the $(R')(O_2)(R')$ fluorite block the (R') layers are displaced relative to one another by the $\frac{1}{2}(\vec{a}+\vec{b})$ translation. The 223 phases have superconducting properties, but the transition temperatures for superconduction in these phases are lower than for the 123 phases ($T_c^{max} = 59$ K).[21] The 223 phases have a tetragonal body-centred cell ($a \approx a_{per}$, $c \approx 7a_{per}$). The model of their structure can be described as of the 14-layer type in which the layers are arranged in the following manner along the *c* axis:

$$\cdots(CuO_2\square_{2-\delta})-(RO)-(R'_2O_2)-(O_2Cu)-(OR)-(\square_{2-\delta}O_\delta Cu)\cdots$$
$$\longleftarrow c/2 \longrightarrow$$

The above schematic arrangement of the layers along the fourfold axis has been confirmed by the determination of the structures of the Ce- and Th-containing 223-phases from single-crystal X-ray diffraction[22] and powder neutron diffraction[23] data. The sites in the fluorite fragment (CN = 8) are populated statistically by the triply charged lanthanide cation and Ce^{4+} (or Th^{4+}). The coordination number of the cations located in the perovskite block depends on the oxygen nonstoichiometry index and is usually close to 10. The coordination polyhedron of the copper atom in the (CuO_2) layer is a tetragonal pyramid extended along the fourfold axis, as in the case of the 123 and T^*-phases. The coordination polyhedron of the copper atom in the $(CuO_\delta\square_{2-\delta})$ layer with $\delta = 0$ is a dumbbell. It is interesting that 223 phases with an ordered arrangement of La^{3+} cations and lanthanides having a smaller radius in the perovskite and fluorite blocks respectively can be obtained. For example, one can obtain $(La_{0.33}Ba_{0.67})_2(Gd_{0.67}Ce_{0.33})_2Cu_3O_{8+\delta}$ [24] and $(La_{0.33}Ba_{0.67})_2(R_{0.67+x}Th_{0.33-x})_2Cu_3O_{8+\delta}$ (R = Nd – Gd, $x = 0$ and 0.17).[22] Such ordering can be achieved as a consequence of the significant differences between the sizes of the vacancies in the given fragments.

The formation of the 223 structure requires the attainment of common dimensions of the perovskite and fluorite blocks in the *ab* plane. The geometrical dimensions of the blocks can be varied by altering their cationic composition. It is noteworthy that the magnitude of the unit cell parameters *a* in compounds with a fluorite block is determined to a large extent by the size of the latter in the *ab* plane, since the highly covalent nature of the bond renders this block the most rigid structural fragment. Table 2 presents as an example a series of 223-phases, the cationic composition of the fluorite blocks of which is the same or similar, whereas the cationic compositions of the perovskite fragments differ quite appreciably. The unit cell parameters *a* of these compounds are very similar, which confirms the conclusion that the linear dimensions of the 223 phases in the *ab* plane are determined primarily by the geometrical dimensions of the cations populating the sites in the fluorite fragment. For the attainment of common dimensions, the change in the composition of the fluorite block should be accompanied by the corresponding change in the cationic composition at the A sites of the perovskite fragment.

The 223 phases containing Ce and Th are isostructural. However, since the ionic radius of Th^{4+} is appreciably larger than that of Ce^{4+}, the cationic compositions of the perovskite fragments of these compounds differ significantly. For example, the 223 phases $R_2Ba_{1.33}Ce_{0.67}Cu_3O_{8+\delta}$ are formed only in systems containing lanthanides from the middle of the series (R = Nd – Eu),[20] whilst the analogous Th-containing phases are

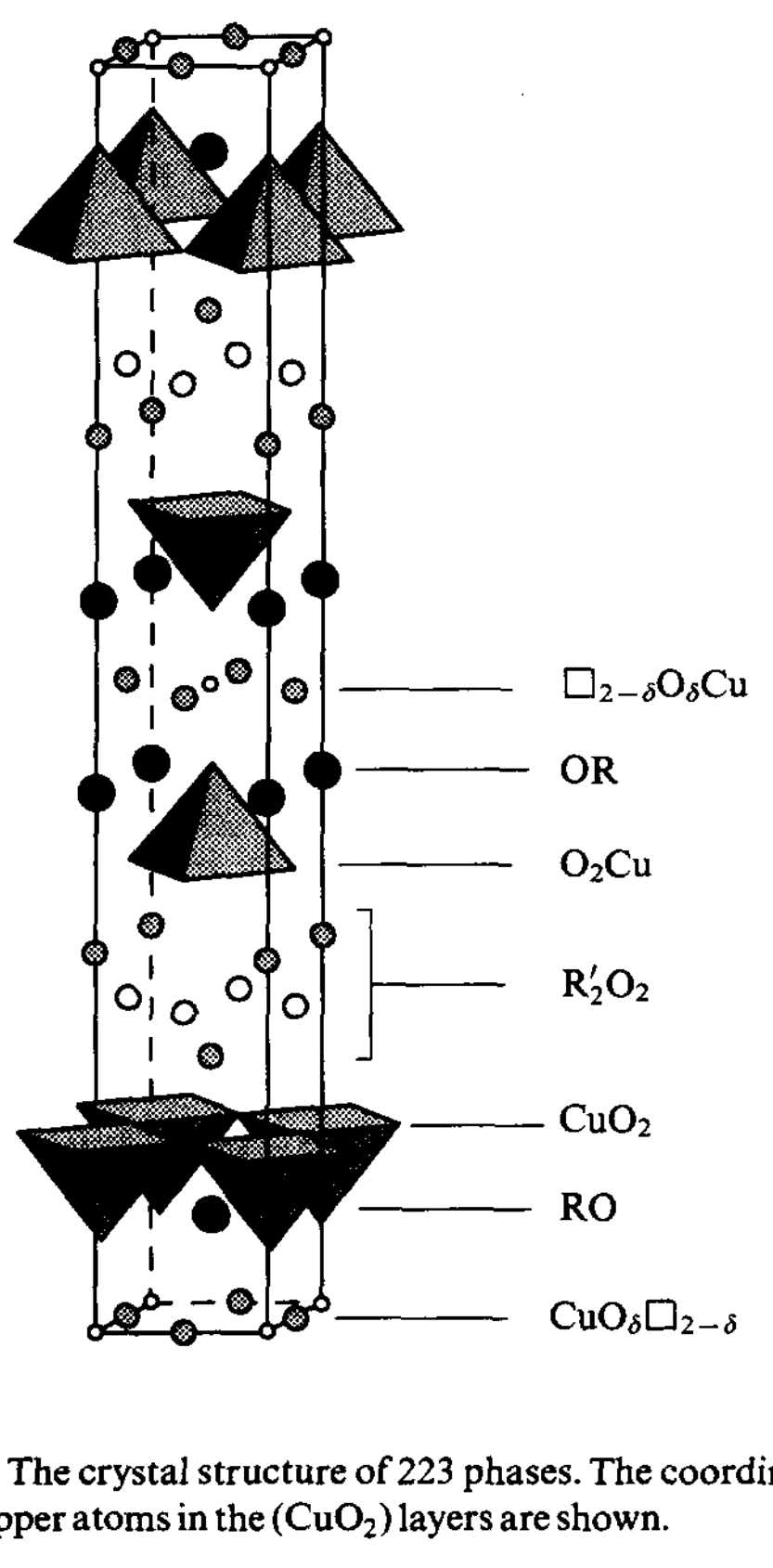


Figure 6. The crystal structure of 223 phases. The coordination polyhedra of the copper atoms in the (CuO_2) layers are shown.

Table 2. The unit cell parameters of 223 phases.

Compound	a/Å	c/Å	Ref.
$(Nd_{0.38}Ba_{0.62})_2(Nd_{0.67}Ce_{0.33})_2Cu_3O_{8.91}$	3.8747(4)	28.599(3)	23
$(Nd_{0.17}Ba_{0.83})_2(Nd_{0.67}Th_{0.33})_2Cu_3O_{8.86}$	3.9071(4)	28.71(2)	22
$(La_{0.33}Ba_{0.67})_2(Nd_{0.67}Th_{0.33})_2Cu_3O_{8.91}$	3.9071(5)	28.762(6)	22
$(Sm_{0.33}Ba_{0.67})_2(Sm_{0.67}Ce_{0.33})_2Cu_3O_{8.79}$	3.8620(8)	28.382(5)	22
$(Sm_{0.33}Ba_{0.67})_2(Sm_{0.67}Th_{0.33})_2Cu_3O_{8+\delta}$	3.8934(6)	28.609(8)	22
$(La_{0.33}Ba_{0.67})_2(Sm_{0.67}Th_{0.33})_2Cu_3O_{8.91}$	3.8935(1)	28.728(4)	22
$(Eu_{0.33}Ba_{0.67})_2(Eu_{0.67}Ce_{0.33})_2Cu_3O_{8+\delta}$	3.8504(1)	28.460(5)	20
$(Eu_{0.10}Sr_{0.90})_2(Eu_{0.70}Ce_{0.30})_2Cu_3O_{8+\delta}$	3.8519(6)	28.157(8)	25
$(La_{0.33}Ba_{0.67})_2(Eu_{0.75}Th_{0.25})_2Cu_3O_{8.78}$	3.8866(9)	28.62(2)	22

formed only in systems with R = La or Pr.[22] The effective radius of the cation in the perovskite fragment of Th-containing compounds must increase compared with the Ce-containing phases. This can be achieved not only by replacing Nd^{3+} by La^{3+} in the perovskite fragment but also by increasing the Ba^{2+} concentration in the cationic sites of the perovskite block.

The 223 phases $(R,M)_2(R',Th)_2Cu_3O_{8+\delta}$ are not formed for M = Sr, whereas in the Ba-containing system such compounds have been obtained for R' = La – Gd. However, when the sites in the fluorite block are populated statistically by the Ce^{4+} and R^{3+} cations, the size of the cationic vacancies diminishes significantly, as a result of which the formation of Sr-containing 223 phases becomes possible in systems with R = Pr – Gd.[25] We may note that the phases with R = Sm and Eu possess superconducting properties, whereas the large Cu – O distance in the (CuO_2) layer in the Th-containing compounds is responsible for the localization of the electronic states. On further contraction of the fluorite fragment for R = Dy – Yb and Y, Ba-containing phases were not obtained, while in the case where M = Sr the 1222 phases, differing from the 223 phases in composition and structure, were produced. The partial or complete substitution of the copper cation in the $(CuO_\delta\square_{2-\delta})$ layer by another cation takes place in the structure of the 1222 phases. The filling of the oxygen sites in this layer is determined by the crystal chemistry of the given cation. Such change in the structure leads to a marked deformation of the CuO_2 layers and to the loss of superconducting properties. On the basis of experiments of this kind, one may conclude that the synthesis of superconducting complex copper oxides with a fluorite fragment requires the presence of Ce^{4+} and $Nd^{3+} - Gd^{3+}$ in the latter, since this leads to the optimum Cu – O distances for the manifestation of superconductivity.

The 1222 phase was first obtained in the Pb – Pr – Sr – Cu – O system.[26] Instead of the $(CuO_\delta\square_{2-\delta})$ layer, its structure contains the $(Pb_{0.5}Cu_{0.5}O_\delta)$ layer in which the anions populate statistically both the sites at the centre of the square $(\frac{1}{2}, \frac{1}{2}, 0)$ and the perovskite sites $(0, \frac{1}{2}, 0)$. The $TlSr_2(Nd,Ce)_2Cu_2O_{8+\delta}$ phase is close to those described above, but the $(CuO_\delta\square_{2-\delta})$ layer in its structure is fully replaced by the (TlO_δ) layer.[27] The compounds $(R_{1.5}Ce_{0.5})Sr_2Cu_2Nb(Ta)O_{10}$ (R = Pr – Eu), the structures of which contain the (NbO_2) or TaO_2 layers instead of the $(CuO_\delta\square_{2-\delta})$ layer, have also been described.[28,29]

There is a possibility also of a further increase in the complexity of the structures of the 223- and 1222-phases as a result of the incorporation in the fluorite fragment of additional (R') and (O_2) layers. In this case, the fluorite block has the composition (R'_3O_4). The 233-phases $Sr_2(R,Ce)_3Cu_3O_{10+\delta}$ [30] and the 1232-phases $(Pb,Cu)Sr_2(R,Ce)_3Cu_2O_{11+\delta}$, as well as $(Tl,Cu)Sr_2.(R,Ce)_3Cu_2O_{11+\delta}$ [31] are derivatives of the 223- and 1222-phases with 'doubled' fluorite fragments.

3. The superconducting mercury-containing family of layered cuprates: $HgBa_2Ca_{n-1}Cu_nO_{2n+2+\delta}$ ($n = 1-4$)

The structures of the Bi-, Tl-, and Pb-containing high-temperature superconductors (HTSC) can be regarded as intergrowth structures of the perovskite and sodium chloride blocks, the Bi^{3+}, Tl^{3+}, and Pb^{2+} cations being located in the NaCl-type fragment. It is noteworthy that the ideal equatorial M – O distance for these cations is to a large extent determined by the Cu – O distance in the CuO_2 layer: $d_{M-O} \approx \sqrt{2}d_{Cu-O}$. However, the calculated values significantly exceed the characteristic values d_{M-O}. As a consequence of this, marked displacements of these cations and oxygen atoms from the ideal positions take place in the (MO) layers in order to diminish the corresponding interatomic distances and the CN of the cations M. The presence of the lone pair in the Bi^{3+} and Pb^{2+} cations also causes their appreciable displacements, required for the formation of an asymmetric coordination environment.

It is possible to synthesise layered cuprates with structures of this kind by employing Hg^{2+} cations, a characteristic feature of which is the dumbbell-like coordination of the oxygen atoms. In this case, the oxygen sites in the layers with mercury atoms may be partly filled or even remain vacant, since the Hg – O bond in this layer must be very weak. Under these conditions, there should be no incompatibility between the dimensions of the structural NaCl and perovskite fragments.

The new layered oxides $HgBa_2CuO_{4+\delta}$ [32], $HgBa_2CaCu_2.O_{6+\delta}$ [33], $HgBa_2Ca_2Cu_3O_{8+\delta}$, and $HgBa_2Ca_3Cu_4O_{10+\delta}$ [34] (the Hg-1201, Hg-1212, Hg-1223, and Hg-1234 phases respectively) have been obtained. These compounds belong to the homologous series of layered cuprates with the general formula $HgBa_2Ca_{n-1}Cu_nO_{2n+2+\delta}$, in which $n = 1 - 4$ (Fig. 7). In the structures of the Hg-1212, Hg-1223, and Hg-1234 phases, two, three, and four (CuO_2) layers, separated by $(Ca\square)^{2+}$, respectively are located in the perovskite block. The NaCl-type fragment has a similar construction in these structures and is characterised by the sequence of layers $(BaO)(HgO_\delta)(BaO)$. The unit cell parameter c in these compounds is determined by the following relation: $c(Å) \approx 9.5 + 3.2\,(n-1)$.

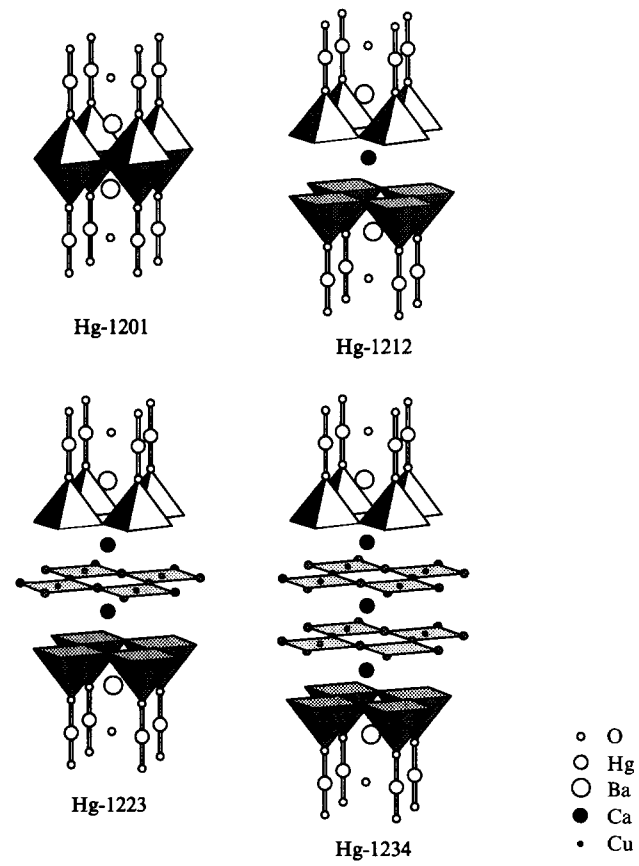


Figure 7. The crystal structures of $HgBa_2Ca_{n-1}Cu_{2n}O_{2+\delta}$ ($n = 1 - 4$).

The results of resistance and magnetic measurements have shown that the Hg-1201, Hg-1212, Hg-1223, and Hg-1234 phases are superconductors with maximum transition temperatures for superconduction of 94, 126, 134, and 126 K respectively.[32,34] The transition temperatures of these compounds can be significantly raised (to 157 K at 235 kbar for Hg-1223) at ultrahigh hydrostatic pressures.[35] The temperature of ~160 K is nowadays the highest at which superconductivity has been recorded. Unfortunately, when the external pressure is removed, the transition temperature falls to the values usual for these compounds.

Neutron and X-ray powder diffraction made it possible to locate the positions of the superstoichiometric oxygen in the Hg-1201 and Hg-1212 structures.[32,33,36,37] It was established that

such oxygen is present in a single layer with mercury atoms and that its content is appreciably less than unity, in contrast to the Tl-containing analogues. Annealing of such phases at different temperatures and partial oxygen pressures leads to a change in the degree of population of this site and hence to an alteration of the concentration of holes in the conduction band and of the transition temperature for superconduction.[32,37]

The family of Hg-containing phases obtained is a promising subject for the investigation of the nature of high-temperature superconductivity in the series of layered cuprates, since high values of T_c are characteristic of these compounds (they are higher than for the Tl-containing phases having a similar cationic composition), this being combined with a fairly simple crystal structure, which is reflected by the absence of modulations and statistical displacements of the atoms and by the high cell symmetry.

III. Intergrowth structures with alternation of fragments along the threefold axis of the perovskite subcell

The structure of the ideal cubic perovskite ABX_3 can be regarded as the spherical close packing of AX_3 layers alternating along the threefold axis. The shift of part of this layer leads to the formation of different types of close packing as regards the layered structure and symmetry, which are also referred to as hexagonal analogues of the perovskite structure. In certain structures of complex perovskite-like oxides with highly layered types of close packing, it is possible to distinguish blocks alternating in an ordered fashion along the c axis (which coincides with the threefold axis of the perovskite subcell), their composition and structures corresponding to those of simpler compounds with less layered packing. Formally, this justifies their consideration as intergrowth structures with alternation of perovskite-like blocks along the threefold axis.

The main geometrical criterion of the possibility of the formation of intergrowth structures is the common dimensions of the initial fragments, i.e. the correspondence of their dimensions in the *ab* plane. In the presence of the same skeleton, formed by close-packed AX_3 layers, the difference between the values of the parameter a is determined by the size of the cations occupying the octahedral vacancies in the close-packed structure.

We shall henceforth consider mainly only compounds in which the close-packed structure is made up of MO_3 (or $MO_{3-\delta}$) layers, where M = Ba, Sr, Ca, or La.

The formation of intergrowth structures is facilitated by the presence of stable structural fragments, the formation of which in the majority of cases is due to the presence of groups of face-linked octahedra arising when part of the layers are displaced by the vector $\frac{1}{3}$, $\frac{2}{3}$, 0 [under these conditions, the 'cubic' (c) layers are transformed into 'hexagonal' layers (h)]. As a result of the presence of common faces in the neighbouring octahedra forming an h-type layer, the distance between the metal cations in these octahedra should correspond to the average thickness of the close-packing layer (for the packing of BaO_3 layers, this range may be 2.2–2.6 Å). This leads to an appreciable electrostatic repulsion of the B cations in the face-linked octahedra. It is useful to discuss the factors stabilising such structural fragments. The electrostatic repulsion of the highly charged B cations may be diminished by the partial population of the B sites by cations with smaller formal charges. This occurs in structures of compounds such as $Ba_4M_3LiO_{12}$ [M = Ta, Nb; 8-layer $(hccc)_2$ packing] and $Ba_5W_3Li_2O_{15}$ [10 layer $(hcccc)_2$ packing].[38–40] In the compound $Ba_5W_3Li_2O_{15}$, chains of vertex-linked octahedra are alternately populated by lithium and tungsten atoms, while pairs of face-linked octahedra are populated statistically: 45% Li + 55% W. A similar motif in the arrangement of the cations is observed also in the structures of the compounds $Ba_4M_3LiO_{12}$. This arrangement of cations leads to minimum repulsion between the highly charged cations M^{6+} or M^{5+}, which is expressed by shortened metal–metal distances (for example, the Ta/Li – Ta/Li distance is 2.258 Å, while the W/Li – W/Li distance is 2.196 Å).

On the other hand, the compounds $Ba_4Ru_3Mo_{12}$ (M = Na, Li) have a different type of distribution of the B cations among the octahedral sites.[41] In the case of the compound $Ba_4Ru_3NaO_{12}$ [8-layer $(hccc)_2$ packing], and $Ba_4Ru_3LiO_{12}$ [6-layer $(hcc)_2$ packing], the face-linked octahedra are populated predominantly by ruthenium, which can be explained by the formation of Ru–Ru bonds.

If the average formal charge of the cations in the B sublattice of the close-packed $A^{2+}O_3$ layers is greater than 4, then, in accordance with the requirement for electroneutrality, cationic vacancies should arise. In the hexagonal analogues of perovskite with cationic vacancies in the B sublattice, the vacancies are located in the blocks of face-linked octahedra. If two types of layers adjoin one another, then there are groups of three face-linked octahedra. When a metal–metal bond cannot be formed owing to electrostatic repulsion forces between cations with a high formal charge, the filling of the middle octahedron is unfavourable and it remains empty. This leads to the formation of phases having the composition $A_nB_{n-1}O_{3n}$, where n is the number of close-packed layers or (for rhombohedral symmetry) the number of layers in one-third of a period. Examples of compounds with such structural organisation are $Ba_5Ta_4O_{15}$ [(hccch) packing][42,43] and $Ba_3Re_2O_9$[$(hch)_3$ packing][44] (Fig. 8), where each octahedron between two type-h layers remains unoccupied by the metal atoms. Members of this homologous series with types of close packing containing 5, 9, 12, 18, and 21 layers are known, all types of packing being trigonal and (apart from the five-layer packing) R-centred.[45–58]

The stability of the chhc fragment justifies the hypothesis that a hexagonal analogue of perovskite exists in which fragments of the $Ba_5Ta_4O_{15}$ and $MZrO_3$ structures (M = Ba, Sr) alternate in

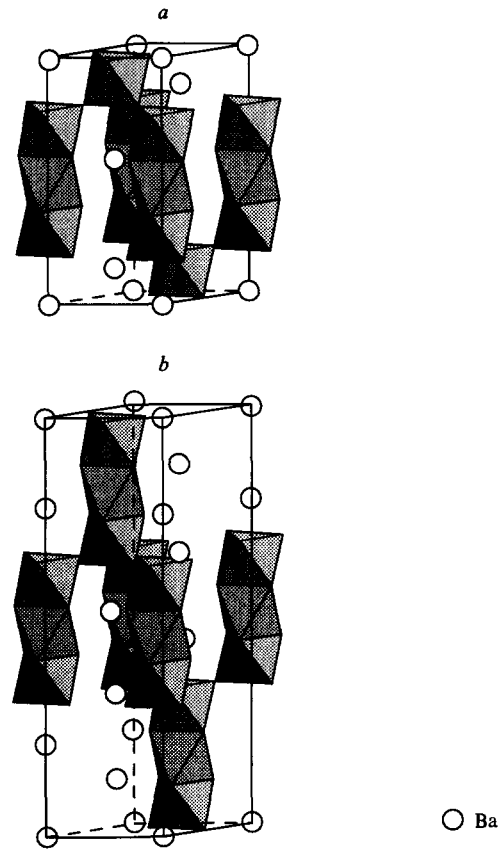


Figure 8. Crystal structures: (*a*) $Ba_5Ta_4O_{15}$; (*b*) $Ba_3Re_2O_9$.

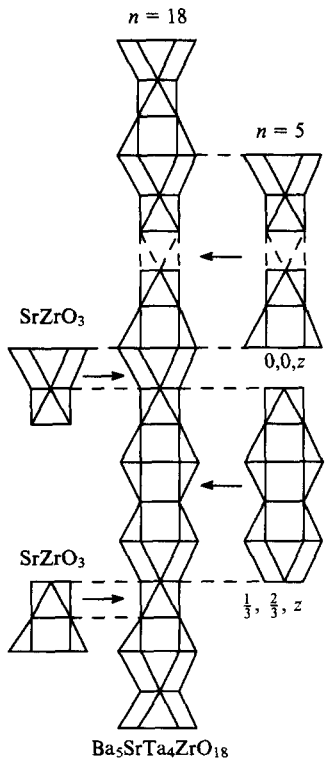


Figure 9. The structure of the compound $Ba_5SrTa_4ZrO_{18}$ resulting from the intergrowth of the $Ba_5Ta_4O_{15}$ and $SrZrO_3$ fragments.

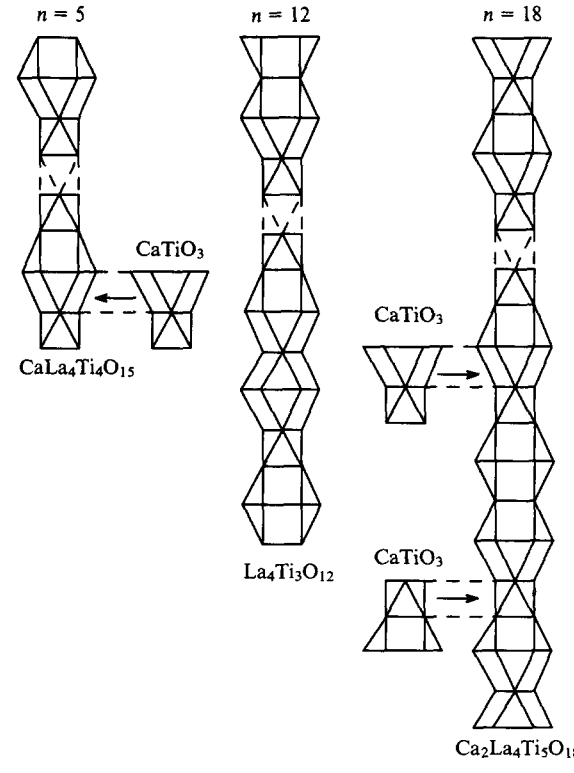


Figure 10. The structures of compounds of the $A_nB_{n-1}O_{3n}$ homologous series resulting from the intergrowth of fragments of the $CaTiO_3$ and $La_4Ti_3O_{12}$ structures.

an ordered fashion along the unit cell *c* axis (Fig. 9). The common dimensions of the fragments in the compound $Ba_5SrTa_4ZrO_{18}$ [(hcccch)$_3$ packing] are attained as a result of the statistical population of the A sites jointly by barium and strontium and of the B sites jointly by tantalum and zirconium, the statistical population of the sites by atoms of two kinds occurring at the block boundaries. Within the $Ba_5Ta_4O_{15}$ blocks, the A sites are occupied only by barium, while the B sites are occupied only by tantalum.

When Ti^{4+} cations are used instead of Zr^{4+}, compounds with structures resulting from the coherent intergrowth of the $Ba_5Ta_4O_{15}$ and $BaTiO_3$ fragments are not formed since the appre-ciably smaller ionic radius of Ti^{4+} (0.605 Å) compared with Zr^{4+} (0.72 Å) gives rise to a lack of common dimensions of the initial structural fragments. Compounds with such structures are formed when barium is replaced by A cations of smaller radius (La, Ca) and when only titanium cations are located in the B sublattice. Obstacles associated with the lack of common dimensions of the fragments do not arise under these conditions and several members of the homologous series are formed — $La_4Ti_3O_{12}$, $CaLa_4Ti_4O_{15}$, and $Ca_2La_4Ti_5O_{18}$.[59] If the 12-layer (hcch)$_3$ packing of the compound $La_4Ti_3O_{12}$ is regarded as a matrix, the subsequent members of the series can be represented as a result of the incorporation in this fragment of a c-type layer corresponding to a fragment of the $CaTiO_3$ perovskite subcell. Structures of this series can be regarded as resulting from intergrowth along the *c* axis of fragments of the $La_4Ti_3O_{12}$ and $CaTiO_3$ packing (Fig. 10). When a single c-type layer is incorporated in the hcch fragment of the initial 12-layer packing of $La_4Ti_3O_{12}$, the compound $CaLa_4Ti_4O_{15}$ with a cell having a P-type symmetry is formed, since the formation of an R-centred cell is impossible in the resulting hccch packing. When two c-type layers are incorporated in the initial fragment, the next member of the homologous series is formed — $Ca_2La_4Ti_5O_{18}$, in the structure of which an 18-layer (hcccch)$_3$ packing is achieved and the symmetry is restored to $R\bar{3}m$. In the case of compounds belonging to this homologous series, an additional factor ensuring the common dimensions of the fragments of the initial types of packing is the joint population of the A sites by lanthanum and calcium atoms. A similar homologous series is formed when the $LaFeO_3$ perovskite fragment is incorporated in the $La_4Ti_3O_{12}$ matrix, two members of this series being known — $La_5FeTi_3O_{15}$ and $La_6Fe_2Ti_3O_{18}$.[60] By using the fact that quadrupole splitting of the Mössbauer signal for Fe(III) in a high-spin state depends only on the degree of distortion of the coordination environment, which is much greater for the octahedra located between the h and c layers owing to the presence of a cationic vacancy, it is possible to show that the iron ions are located predominantly in the octahedral vacancies within the perovskite blocks. Such distribution of the cations among the B sites agrees well with the intergrowth structures model.

Apart from the structures of compounds which are formed as a result of an increase in the number of type $LaTiO_3$ blocks, a series of phases with different ratios of structural blocks exist along the $La_4Ti_3O_{12} - LaTiO_3$ section.[61] The simplest example of such phases is the oxide $La_9Ti_7O_{27}$. The structure of this compound can be represented as a result of the intergrowth of $2 \times La_4Ti_3O_{12} + LaTiO_3$ blocks. Formally, this structure can be more conveniently considered as a result of the intergrowth of higher homologues ($n \leqslant 6$): $La_4Ti_3O_{12} + La_5Ti_4O_{15}$ (or ...4545..., in terms of the number of blocks). The results of detailed microscopic studies of the phases formed along the $La_4Ti_3O_{12} - LaTiO_3$ section have been published.[62] The authors demonstrated the existence of a large number of ordered polytypes — $La_{11}Ti_9O_{33}$: $2 \times La_4Ti_3O_{12} + 3 \times LaTiO_3$ or ...5656...; $La_{13}.Ti_{10}O_{39}$: $3 \times La_4Ti_3O_{12} + LaTiO_3$ or ...445...; etc. However, in practice, it is difficult to synthesise these compounds in a pure form because of the decrease in the energy differences between the homologues with increase in their ordinal number.

The population by B cations of the entire group of three face-linked octahedra is possible in the presence of an additional stabilising factor such as the formation of metal–metal bonds. Thus, in the $BaRuO_3$ structure, where the valence state

of ruthenium permits the formation of Ru–Ru bonds, all three adjacent octahedra are populated with formation of the $[Ru_3O_{12}]$ clusters.[63] The Ru–Ru distance in this structure is 2.55 Å.

When the chhc structural fragment cannot be stabilised, the incorporation of the cation in the middle of the three face-linked octahedra is unfavourable as a result of the short metal–metal distances arising under these conditions and the strong electrostatic repulsion and leads to a change in the type of close packing and the formation of hexagonal analogues of perovskite with the joint population of the B sites by cations and vacancies. Thus a trigonal primitive hccch close packing arises in the compound $Ba_5Ta_4O_{15}$. The heterovalent substitution of Ta^{5+} by Ti^{4+} leads to the appearance of an additional amount of B cations,[64] which exerts a decisive influence on the type of close packing produced. On passing from $Ba_5Ta_4O_{15}$ to $Ba_{10}Ta_{8-0.8x}Ti_xO_{30}$ solid solutions [$(hcccc)_2$ close packing, $0.6 \leqslant x \leqslant 1.2$], the type of close packing changes, the unit cell parameter c is doubled, and the symmetry is altered from $P\bar{3}m1$ to $P6_3/mmc$. This is accompanied by the delocalisation of the cationic vacancies and the joint population of the cationic sites by tantalum atoms and vacancies takes place in the chc structural fragment present in the $Ba_{10}Ta_{7.04}Ti_{1.2}O_{30}$ structure.

If the sum of the formal charges on the A and B cations is less than six, the formation of anion-deficient hexagonal analogues of perovskite having the composition $ABO_{3-\delta}$ is possible. In this case, the formation of stable structural fragments may be associated with the location of anionic vacancies outside the B cations for which CN < 6.

A group of hexagonal perovskite-like oxides is known where the appearance of anionic vacancies is induced by the introduction of aluminium atoms into the B sublattice. The structure of β-Ba_2RAlO_5 (R = Sc, In) (Fig. 11) is based on the eight-layer $(hccc)_2$ close packing.[65,66] The arrangement of the scandium and aluminium atoms is entirely ordered, the B-sites in the vertex-linked octahedra being populated by scandium alone. The ordered population of the B sites leads to the location of the oxygen atom on the 6_3 axis and the formation of a tetrahedral environment around the aluminium atoms. The group of two face-linked octahedra is then transformed into a group made up of two Al_2O_7 tetrahedra linked via the vertices. The ordering of the scandium, aluminium, and oxygen atoms leads also to a change in the coordination polyhedra around the barium atoms. One-fourth of the barium atoms are located in an almost ideal cubooctahedron. For another fourth of barium atoms, the appearance and ordering of the anionic vacancies lead to the removal of three out of the six oxygen atoms of the equatorial environment of the barium atoms, the three remaining oxygen atoms being displaced from the ideal positions (the Ba – O distance is 3.345 Å) and building up the coordination polyhedron of the barium atom to a truncated trigonal bipyramid (CN = 9). For the remaining half of the barium atoms, the displacement of the oxygen atoms in the $BaO\square_2$ layer leads to the appearance of a kind of open polyhedron in the form of a nonagon produced after the removal of the oxygen atoms making up the common face of the cubooctahedra in the h layer.

The fragments of the β-Ba_2RAlO_5 and $Ba(Sr)ZrO_3$ close packing (type c layers) in the structures of compounds with the general composition $Ba_{5-y}Sr_yR_{2-x}Al_2Zr_{1+x}O_{13+x/2}$ (R = Sc, In, Y, Gd–Lu) having a 10-layer close packing of BaO_{3-x} $(hcccc)_2$ layers alternating along the sixfold axis may be regarded as intergrowth structures (Fig. 12).[67] We may note that the compounds Ba_2RAlO_5 (R = Nd – Lu, Y) crystallise in the monoclinic system. When the ratio of the structural fragments corresponds to $2 \times (Ba_2RAlO_5) + (BaZrO_3)$, the ideal composition of the compounds is described by the formula $Ba_5R_2Al_2ZrO_{13}$. The establishment of common dimensions of the fragments in the given instance should be facilitated by the joint population of the B sites by zirconium and R^{3+} cations.

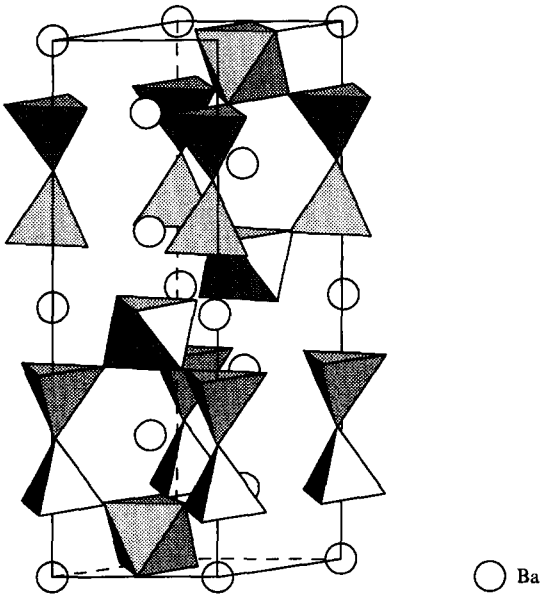


Figure 11. The crystal structure of β-Ba_2ScAlO_5.

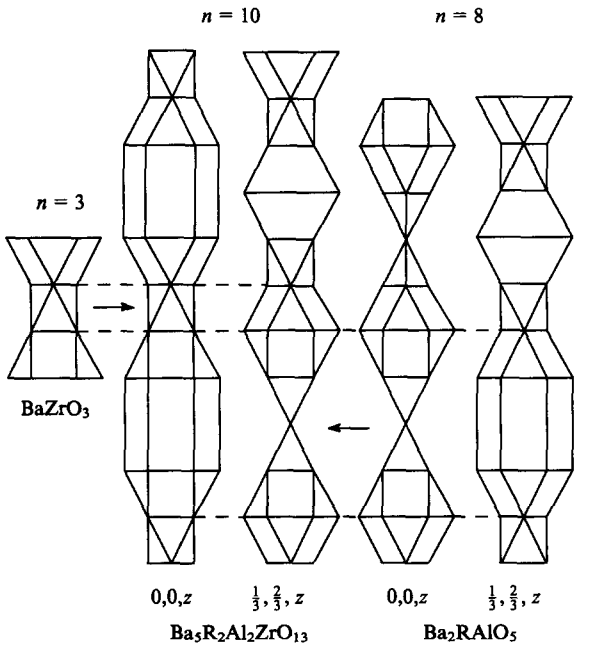


Figure 12. The structure of the compounds $Ba_5R_2Al_2ZrO_{13}$ resulting from the intergrowth of the Ba_2RAlO_5 and $BaZrO_3$ fragments.

The ionic radius of the R^{3+} cations exerts a significant influence on the stability of the compounds formed. Thus the formation of the compounds $Ba_5R_2Al_2ZrO_{13}$ was not observed for R = La – Eu. In this case, the radius of R^{3+} is too large for the accommodation of the ion in the octahedral vacancies within the close-packed BaO_{3-x} layers.

The significant difference between the ionic radii of R^{3+} (R = Gd – Lu; radii in the range 0.94–0.95 Å) and Zr^{4+} (0.72 Å) gives rise to the possibility of the existence of an ordered structure. The lanthanide cations are located in the octahedral vacancies of the type-β-Ba_2RAlO_5 block, whereas the Zr^{4+} cations are in the

$BaZrO_3$ block. In contrast to the $Ba_5R_2Al_2ZrO_{13}$ structures (R = Gd – Lu, Y), the structure of the Sc-containing compound is more disordered. In this structure, Sc^{3+} and Zr^{4+} occupy jointly the octahedral vacancies, which can be accounted for by the similarity of their ionic radii: 0.73 and 0.72 Å respectively. As a result of the statistical distribution, the cationic composition of the compound differs from the ideal composition and is expressed by the formula $Ba_5Sc_{1.33}Al_2Zr_{1.67}O_{13.33}$.

As in the β-Ba_2ScAlO_5 structure, in the $Ba_5R_2Al_2ZrO_{13}$ structures the oxygen vacancies are located in the h-type layers, which have the composition $BaO\square_2$. The remaining oxygen atom in this layer occupies a double position on the 6_3 axis, forming a common vertex of two Al_2O_7 tetrahedra. Under these conditions, some of the barium atoms achieve the same coordination environment as in the β-Ba_2ScAlO_5 structure. The change in the cationic composition following the substitution of some of the scandium atoms by zirconium atoms leads to the appearance of excess oxygen (compared with the ideal composition) and the composition of the h-type layer becomes $BaO_{1.33}\square_{1.67}$. The stable tetrahedral environment of the aluminium atoms prevents the delocalisation of the oxygen atom in the $\frac{1}{3}$, $\frac{2}{3}$, $\frac{1}{4}$ position and in the case of $Ba_5Sc_{1.33}Al_2Zr_{1.67}O_{13.33}$ the additional oxygen atom occupies the 0, 0, $\frac{1}{4}$ position, building up the nona-coordination polyhedron of the barium atoms to a decagon.

A characteristic feature of the crystal structure of $Ba_5In_2Al_2ZrO_{13}$ is the joint population of the B sites in the chc close packing fragment by indium and aluminium atoms, which is the cause of the delocalisation of the oxygen atom in the $\frac{1}{3}$, $\frac{2}{3}$, $\frac{1}{4}$ position. However, the compound with this structure is apparently metastable and has been obtained only on fusion of the specimen.

It is possible to distinguish three cases of the distribution of the cations among the B sites, which leads to three different types of location of the oxygen atoms in the BaO_{3-x} layers in the structures of the complex oxides $Ba_{5-y}Sr_yR_{2-x}Al_2Zr_{1+x}O_{13+x/2}$:

(1) the B sites in the chc fragment are occupied only by aluminium: the x, y, $\frac{1}{4}$ and x, y, $\frac{3}{4}$ layers have the composition $BaO\square_2$ and the arrangement of the oxygen atoms and of the anionic vacancies is fully ordered (the crystal structures of $Ba_5R_2Al_2ZrO_{13}$; R = Gd – Lu, Y);

(2) the B sites in the chc fragment are occupied statistically by atoms with stable octahedral and tetrahedral coordinations: the anion-deficient layers have the composition $BaO\square_2$ and the disposition of the oxygen atoms and the anionic vacancies is disordered (the crystal structure of $Ba_5In_2Al_2ZrO_{13}$);

(3) following the partial substitution of the R^{3+} cations by Zr^{4+}, the B positions in the chc fragments are occupied only by aluminium; the anion-deficient layers have the composition $BaO_{1.33}\square_{1.67}$ and the arrangement of the oxygen atoms is partly ordered (the crystal structure of $Ba_5Sc_{1.33}Al_2Zr_{1.67}O_{13.33}$).

In the cases examined above, the intergrowth structures are formed when the 'cubic' ABO_3 layers are incorporated in a multilayer close-packed structure. However, there exist hexagonal perovskites, where structurally isolated blocks, consisting of several 'cubic' and 'hexagonal' layers, alternate along the c axis.

The identical parameters a for the compounds $Ba_3Sc_4O_9$ [69–72] and β-Ba_2ScAlO_5 (5.794 Å) create ideal conditions for the formation of intergrowth structures. High-resolution electron microscope studies indicate the formation of two homologous series based on these compounds.[73,74] The compounds of the first series have the composition $Ba_{3n+8}Sc_{4n+4}Al_4O_{9n+20}$ (n = 2, 3, ...) (or, in a clearer form, $n \times Ba_3Sc_4O_9 + 2 \times Ba_4Sc_2Al_2O_{10}$). It is easily seen that for $n = 2$ the formula of the compound is $Ba_7Sc_6Al_2O_{19}$ (Fig. 13) and each succeeding member of the series is formed after the incorporation of an additional $Ba_3Sc_4O_9$ fragment. Compounds of the second series have the formula $Ba_{2n+3}Sc_{n+4}Al_nO_{5n+9}$ (n = 2, 3, ...) (or $Ba_3Sc_4O_9 + n \times Ba_4Sc_2Al_2O_{19}$), which is obtained following an increase in the number of $Ba_4Sc_2Al_2O_{10}$ blocks in the $Ba_7Sc_6Al_2O_{19}$ structure.

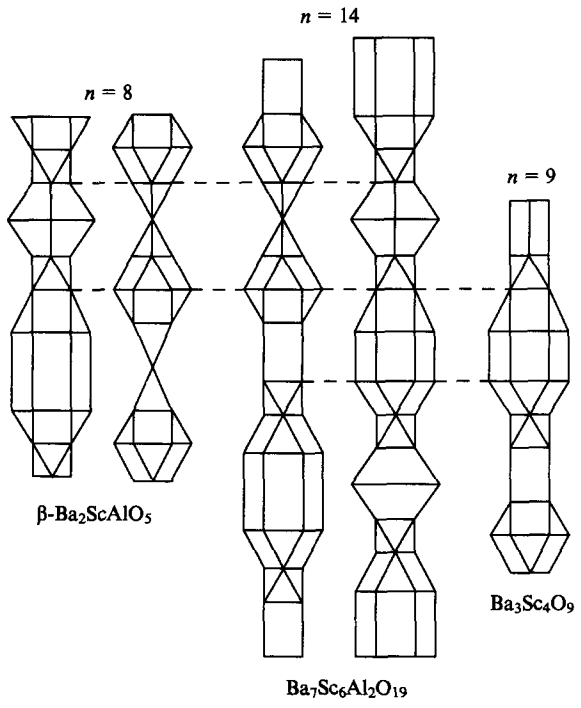


Figure 13. The structure of the compound $Ba_7Sc_6Al_2O_{19}$ resulting from the intergrowth of the β-Ba_2ScAlO_5 and $Ba_3Sc_4O_9$ fragments.

It is noteworthy that the members of homologous series with $n > 3$ were hardly observed or were present in the form of irregularly alternating sequences.

Barium ferrites form yet another group of hexagonal perovskites with intergrowth structures.[75,76] This family of compounds is obtained on 'by intergrowth' of $BaFe_{12}O_{19}$ structural blocks [M-type; $P6_3mmc$ (cchcc)$_2$] with $Ba_2M^{II}Fe_{12}O_{22}$ [Y-type: $R\bar{3}m$ (cchhcc)$_3$] or $M^{II}_2Fe_4O_8$ (M^{II} = Mg, Zn, Co) (*S*-type: $Fd3m$ spinel structure) in different proportions and sequences. The so called series of compounds M_2Y_n is formed along the $BaFe_{12}O_{19} - Ba_2M^{II}Fe_{12}O_{22}$ section. If the repeating parts of the sequences are denoted by M and Y, the compounds obtained have the composition M_2Y_n. Ordered phases with the ratios M : Y ranging from 2 : 1 to 2 : 11 have been obtained for them. Phases with even more complex ratios of the fragments have been discovered with the aid of high-resolution electron microscopy.

Compounds in the structures of which blocks having similar constructions and compositions alternate were described above. Thus a single principle governing the disposition of the cations among the crystallographic sites is maintained in all the structures based on the close packing of AO_3 layers. However, there are examples of crystal structures resulting from the intergrowth of blocks, which have at first sight both different compositions and constructions. Such compounds are chloro-oxoruthenates. Their structures are made up of fragments alternating in an ordered manner, one of which has the composition $[Ba_2Cl_2]^{2+}$, while the other is a fragment of the close-packed BaO_3 layers.[77–79] The structure of $Ba_5RuTaO_9Cl_2$ (Fig. 14) is made up of the close-packed fragments separated by two $[BaCl]^+$ layers, each of which is constructed in the same way as the $BaO\square_2$ layer in the compounds $Ba_5R_2Al_2ZrO_{13}$. Some of the barium atoms have under these conditions a coordination environment with CN < 12, where some of the oxygen atoms have been replaced by chlorine.

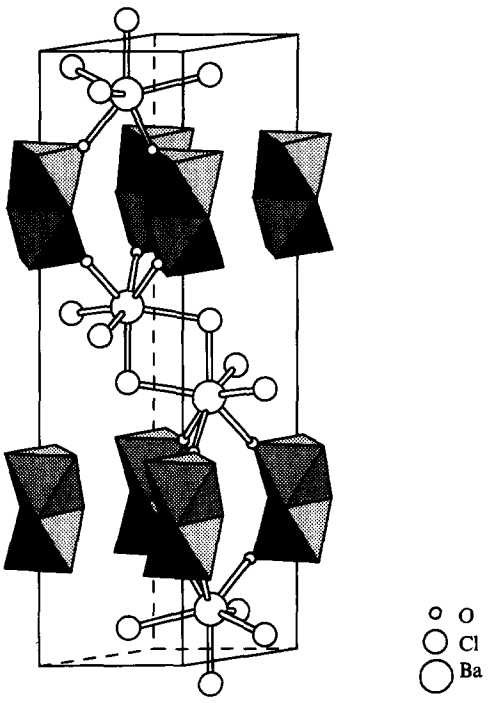


Figure 14. The crystal structure of $Ba_5RuTaO_9Cl_2$.

IV. Conclusion

The value of the prediction of the composition of new phases with high-temperature superconducting properties has been demonstrated in relation to complex copper oxides. New ternary copper, mercury, and barium oxides having high transition temperatures for superconduction have been obtained with the aid of this principle. This is a consequence of the fact that in this instance the CuO_2 layers are least distorted. The replacement of mercury by thallium, bismuth, or lead decreases T_c owing to the distortions of the CuO_2 layer under the influence of the lone pairs of the cations of the given elements.

The formation of oxygen vacancies in coherent intergrowth structures containing blocks of the NaCl and CaF_2 types together with CuO_2 layers alters the type of coordination from the octahedron to the tetragonal pyramid or a dumbbell, depending on the electronic structures of the corresponding ions.

A series of phases, differing in the layered structure and symmetry in the close packing, arise in compounds with alternation of structural blocks along the threefold axis of the perovskite structure (which is a prototype structure). In this case, the common dimensions of the fragments are achieved by altering the cationic composition in the A and B sublattices of the initial structural blocks.

References

1. A Wells *Structural Inorganic Chemistry* Vol. 2 (Oxford: Oxford University Press) (Translated into Russian; Moscow: Mir, 1988) p. 695
2. P Ganguli, C N R Rao *J. Solid State Chem.* **53** 193 (1984)
3. B Grande, H K Müller-Buschbaum, M Sweizer *Z. Anorg. Allg. Chem.* **428** 120 (1977)
4. N Nguyen, J Choisnet, M Hervieu, B Raveau *J. Solid State Chem.* **39** 120 (1981)
5. M Onoda, S Shamoto, M Sato, S Hosoya *Jpn. J. Appl. Phys.* **26** 363 (1987)
6. K Oh-ishi, M Kikuchi, M Syono, N Kobayashi, T Sasaoka, T Matsuhira, Y Muto, H Yamauchi *Jpn. J. Appl. Phys.* **27** L 1449 (1988)
7. H K Müller-Buschbaum, W Wollschlager *Z. Anorg. Allg. Chem.* **414** 76 (1975)
8. F Izumi, Y Matsui, H Takagi, S Uchida, Y Tokura, H Asano *Physica C* **158** 433 (1989)
9. M J Rosseinsky, K Prassides, P Day *Physica C* **161** 21 (1989)
10. Y Tokura, H Takagi, S Uchida *Nature (London)* **337** 345 (1989)
11. N Kimizuka, E Takayama, S Horiuchi *J. Solid State Chem.* **42** 322 (1982)
12. P Bordet, J J Capponi, C Chaillout, D Chateigner, J Chenavas, Th Fournier, J L Hodeau, M Marezio, M Perroux, G Thomas, A Varela *Physica C* **193** 178 (1992)
13. Y Y Xue, P H Hor, R L Meng, Y K Tao, Y Y Sun, F Huang, L Gao, C W Chu *Physica C* **165** 357 (1990)
14. Y Maeno, F Lichtenberg, T Williams, J Karpinski, J G Bednorz *Jpn. J. Appl. Phys.* **28** L926 (1989)
15. S-W Cheong, Z Fisk, J D Thompson, R B Schwartz *Physica C* **159** 407 (1989)
16. E M Kopnin, E V Antipov, L M Kovba, P E Kazin, V A Rybachuk, V V Moshchalkov, A E Kachanovskii *Sverkhprovodn: Fiz., Khim., Tekh.* **5** 530 (1992)
17. J F Bringley, S S Trail, B A Scott *J. Solid State Chem.* **86** 310 (1990)
18. B Dubois, G Dahlenne, F Yviire, A Revcolevtschi *J. Am. Ceram. Soc.* **69** C6 (1986)
19. J F Bringley, S S Trail, B A Scott *J. Solid State Chem.* **88** 590 (1990)
20. H Sawa, K Obara, J Akimitsu, Y Matsui, S Horiuchi *J. Phys. Soc. Jpn.* **58** 2252 (1989)
21. S Ikegawa, T Wada, A Ichinose, T Yamashita,T Sakurai, Y Yaegashi, T Kaneko, M Kosuge, H Yamauchi, S Tanaka *Phys. Rev. B, Cond. Matter.* **41** 11673 (1990)
22. E M Kopnin, A V Mironov, E V Antipov, L M Kovba, L G Akselrud, I G Muttik, V V Moshchalkov *J. Solid State Chem.* **100** 30 (1992)
23. F Izumi, H Kito, H Sawa, J Akimitsu, H Asano *Physica C* **160** 235 (1989)
24. T Wada, A Ichinose, Y Yaegashi, H Yamauchi, S Tanaka *Phys. Rev. B, Cond. Matter.* **41** 1984 (1990)
25. E M Kopnin, A L Kharlanov, I Bryntse, E V Antipov *Physica C* **219** 47 (1994)
26. S Adachi, O Iuone, S Kawashima, H Adachi, Y Ichikawa, K Setsune, K Wasa *Physica C* **168** 1 (1990)
27. R S Liu, M Hervieu, C Michel, A Maignan, C Martin, B Raveau, P P Edwards *Physica C* **197** 131 (1992)
28. L Rukang, Z Yingjie, X Cheng, C Zuyao, Q Yitai, Chen Gao *J. Solid State Chem.* **94** 206 (1991)
29. T J Goodwin, H B Radousky, R N Shelton *Physica C* **204** 212 (1992)
30. T Wada, A Ichinose, H Yamauchi, S Tanaka *Physica C* **171** 344 (1990)
31. T Wada, A Ichinose, F Izumi, A Nara, H Yamauchi, H Asano, S Tanaka *Physica C* **179** 455 (1991)
32. S N Putilin, E V Antipov, O Chmaissem, M Marezio *Nature (London)* **362** 226 (1993)
33. S N Putilin, E V Antipov, M Marezio *Physica C* **212** 266 (1993)
34. E V Antipov, S M Loureiro, C Chaillout, J J Capponi, P Bordet, J L Tholence, S N Putilin, M Marezio *Physica C* **215** 1 (1993)
35. M Nunez-Requeiro, J L Tholence, E V Antipov, J J Capponi, M Marezio *Science* **262** 97 (1993)
36. O Chmaissem, Q Huang, S N Putilin, M Marezio, A Santoro *Physica C* **212** 259 (1993)
37. S M Loureiro, E V Antipov, J L Tholence, J J Capponi, O Chmaissem, Q Huang, M Marezio *Physica C* **217** 253 (1993)
38. T Negas, R S Roth, H S Parker, W S Brower *J. Solid State Chem.* **8** 1 (1973)
39. B M Collins, A J Jacobson, B E F Fender *J. Solid State Chem.* **10** 29 (1974)
40. A J Jacobson, B M Collins, B E F Fender *Acta Crystallogr., Sect. B, Struct. Crystallogr.* **30** 816 (1974)
41. P D Battle, S H Kim, A V Powell *J. Solid State Chem.* **101** 161 (1992)
42. F Galasso, L Katz *Acta Crystallogr., Sect. B* **14** 647 (1961)
43. J Shannon, L Katz *Acta Crystallogr., Sect. B, Struct. Crystallogr.* **26** 102 (1970)

44. C Calvo, H N Ng, B L Chamberland *Inorg. Chem.* **17** 699 (1978)
45. S Kemmler-Sack, I Jooss *Z. Anorg. Allg. Chem.* **439** 232 (1978)
46. S Kemmler-Sack, W Wischert, U Treiber *Z. Anorg. Allg. Chem.* **444** 190 (1978)
47. W Wischert, H-J Schittenhelm, S Kemmler-Sack *Z. Anorg. Allg. Chem.* **439** 250 (1978)
48. W Wischert, H-J Schittenhelm, S Kemmler-Sack *Z. Anorg. Allg. Chem.* **448** 119 (1979)
49. S Kemmler-Sack *Z. Anorg. Allg. Chem.* **461** 142 (1980)
50. H-J Rother, A Fadini, S Kemmler-Sack *Z. Anorg. Allg. Chem.* **463** 137 (1980)
51. H-J Rother, S Kemmler-Sack *Z. Anorg. Allg. Chem.* **465** 179 (1980)
52. S Kemmler-Sack *Z. Anorg. Allg. Chem.* **457** 157 (1979)
53. H-J Rother, S Kemmler-Sack, U Treiber, W-R Cyris *Z. Anorg. Allg. Chem.* **466** 131 (1980)
54. M Hermann, S Kemmler-Sack *Z. Anorg. Allg. Chem.* **470** 113 (1980)
55. S Kemmler-Sack *Z. Anorg. Allg. Chem.* **453** 163 (1979)
56. S Kemmler-Sack, M Hermann *Z. Anorg. Allg. Chem.* **480** 171 (1981)
57. H-J Schittenhelm, S Kemmler-Sack *Z. Anorg. Allg. Chem.* **465** 183 (1980)
58. B Mossner, S Kemmler-Sack *J. Less-Commun. Met.* **120** 287 (1986)
59. M German, L M Kovba *Zh. Neorg. Khim.* **30** 317 (1985)
60. M German, L M Kovba *Zh. Neorg. Khim.* **28** 2377 (1983)
61. R Bontchev, B Darriet, J Darriet, F Weill, G Van Tendeloo, S Amelinckx *Eur. J. Solid State Chem.* **30** 521 (1993)
62. G Van Tendeloo, S Amelinckx, B Darriet, R Bontchev, J Darriet, F Weill *J. Solid State Chem.* **108** 336 (1994)
63. P C Donohue, L Katz, R Ward *Inorg. Chem.* **4** 306 (1965)
64. R V Shpanchenko, L Nistor, G Van Tendeloo, J Van Landuyt, S Amelinckx, A M Abakumov, E V Antipov, L M Kovba *J. Solid State Chem.* **114** 560 (1995)
65. R V Shpanchenko, E V Antipov, L N Lykova, L M Kovba *Vestn. Mosk. Univ., Ser. 2: Khim.* **31** 555 (1990)
66. Hk Müller-Buschbaum, M Abed *Z. Anorg. Allg. Chem.* **591** 174 (1990)
67. R Shpanchenko, A M Abakumov, E V Antipov, L Nistor, G Van Tendeloo, S Amelinckx *J. Solid State Chem.* (1995) (in the press)
68. R V Shpanchenko, A M Abakumov, E V Antipov, L M Kovba *J. Alloys Compd. (Switzerland)* **206** 185 (1994)
69. Hk Müller-Buschbaum, M Scheikowski *Z. Anorg. Allg. Chem.* **591** 181 (1990)
70. G Von Brauer, H Kristen *Z. Anorg. Allg. Chem.* **462** 35 (1980)
71. L M Kovba, M V Paromova *Vestn. Mosk. Univ., Ser. 2: Khim.* 621 (1970)
72. J Kruger, Hk Müller-Buschbaum *Z. Anorg. Allg. Chem.* **512** 59 (1984)
73. R V Shpanchenko, E V Antipov, M V Paromova, L M Kovba *Zh. Neorg. Khim.* **36** 1402 (1991)
74. R Shpanchenko, L Nistor, G Van Tendeloo, S Amelinckx, E Antipov, L Kovba *J. Solid State Chem.* **113** 193 (1994)
75. J Van Landuyt, G Van Tendeloo, S Amelinckx, in *Crystal Growth and Characterisation of Polytypes* (Oxford: Pergamon Press, 1983) p. 365
76. J Van Landuyt, S Amelinckx, J A Kohn, D W Eckart *J. Solid State Chem.* **9** 103 (1974)
77. M Neubacher, Hk Müller-Buschbaum *Z. Anorg. Allg. Chem.* **602** 143 (1991)
78. J Wilkens, Hk Müller-Buschbaum *J. Less-Common. Met.* **171** 255 (1991)
79. J Wilkens, Hk Müller-Buschbaum *Acta Chem. Scand.* **45** 812 (1991)